Defence Science Journal, Vol. 59, No. 2, March 2009, pp. 106-112
© 2009, DESIDOC

# Development of Eddy Current Test Procedure for Non-destructive Detection of Fatigue Cracks and Corrosion in Rivets of Air-intake Structures

B. Sasi, B.P.C. Rao, T. Jayakumar, and Baldev Raj

*Indira Gandhi Centre for Atomic Research, Kalpakkam–603 102*

**ABSTRACT**

Non-destructive detection of defects in countersunk of rivets in multi-layer air-intake structures is essential for ensuring structural integrity and flight safety. This paper presents an eddy current test procedure developed for reliable detection of simulated fatigue cracks and corrosion products in rivets of air-intake structures. This procedure is capable of reliably detecting 0.25 mm deep defects in 4 mm dia rivets and 0.75 mm deep defects in 5 mm dia rivets. Further, it is not influenced by thickness of the multilayers.

**Keywords:** Air-intake structures, rivets, eddy currents, fatigue crack, hidden corrosion

## 1. INTRODUCTION

Non-destructive testing (NDT) of critical components of aircraft, especially airframes and aero engines, is essential for ensuring structural integrity and flight safety. The NDT of aircraft in service has assumed greater importance after the Aloha accident of 1988 and special emphasis has been placed on detection of fatigue cracks and hidden corrosion in airframe structures and in rivet heads[1,2]. Among various NDT techniques, visual inspection using boroscopes and fibroscopes is routinely carried out. This technique has limitation for detection of sub-surface defects and can not be used for sizing defects[3]. Eddy current (EC) testing is well-suited for testing airframes and aero engine discs and is routinely used during quality assurance, maintenance, and life extension of aircraft[4]. EC technique is known for its ease, versatality, speed, and non-contact nature. Several developments have taken place in the recent years for applying this technique to riveted panels in aircraft structures. Sliding probes are developed for detection of fatigue cracks in the skins of the riveted panels[5]. For detection of fatigue cracks around the rivet heads and measurement of residual stresses, self-nulling rotating probes are developed[6]. To detect short-fatigue cracks under the skins of rivet heads, as a part of damage tolerance assessment, Hegemaier[7], *et al.*, studied the performance of various eddy current systems and probes using electro-discharge machining (EDM) notches.

In the recent past, extensive investigations on failures occurred in MiG-21 aircraft revealed that the failures were caused primarily due to the tear-off of rivet heads in the airframe structures, thus disturbing the structural integrity of air-intake structures. The tear-off of rivet heads was attributed to the presence of fatigue cracks in the countersunk regions of the rivet heads rather than in the fuselage skins. The sharp edges in the skins provide high stress concentration at the countersunk region of the rivet heads and promote initiation of fatigue cracks. Small fatigue cracks grow with time radially through the rivet head and cause the tear-off, resulting in catastrophic failures. Typical portion of a riveted structure from a Cat-E aircraft is shown in Fig. 1. Van der Walde[8], *et al.*, studied the corrosion-assisted fatigue crack in 2024-T3 aluminium sheets for different cyclic loadings, and found that crack initiation was predominantly due to stress amplification at corroded regions and joining of microcracks. Early and reliable detection of fatigue cracks and corrosion in the countersunk region of the rivet heads through periodic NDT is essential and is expected to ensure flight safety.

Development of eddy current test procedure for detection of fatigue cracks as well as corrosion in countersunk region of the rivet heads is desired. In this direction, studies have been focused on detection of cracks in rivet heads, and to examine the influence of corrosion products in defect regions. Further, studies have also been carried out to study the effect of thickness of multilayers on the eddy current procedure. In this direction, riveted multilayer aircraft structures with machined grooves in the countersunk region of the rivet heads, simulating the fatigue cracks and with a few grooves filled with aluminium powder in a glue matrix (simulating corrosion) have been studied. This paper discusses details of these experimental studies, optimisation of test parameters, and results of the investigations towards development of an effective procedure for NDT of air-intake structures.

## 2. PRINCIPLES OF EDDY CURRENT TESTING

The EC testing works on the principles of electromagnetic induction and involves measurement of change in coil

Received 14 May 2008

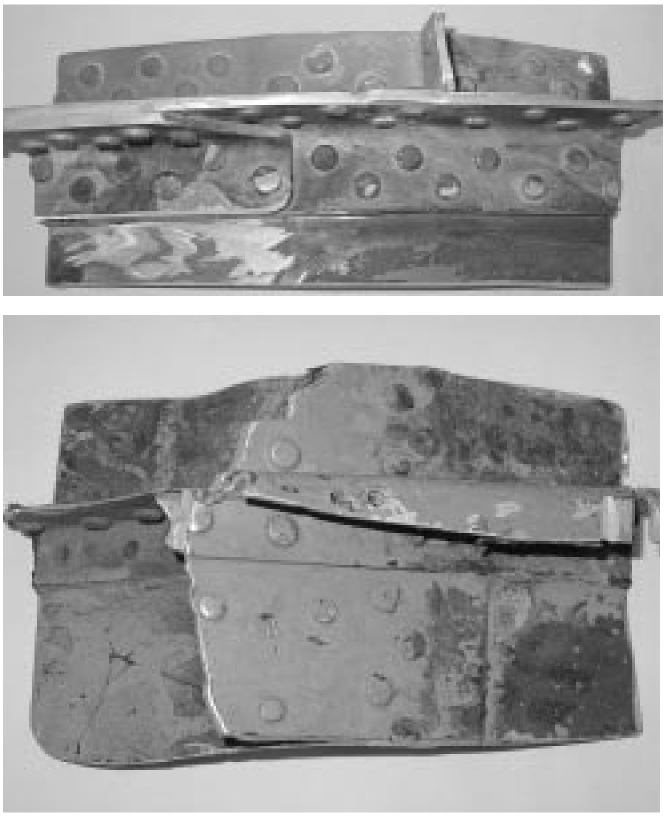

**Figure 1. Photographs of a portion of riveted panels from a failed aircraft (Cat-E).**

impedance that arises due to perturbation of eddy currents at defect regions. In EC testing, an alternating current (frequency, *f*, in the range of 50 Hz –5 MHz) is made to flow in a coil (also called probe) which in turn produces an alternating magnetic field around it. When the coil is brought close to an electrically-conducting material, eddy currents are induced in the material. These eddy currents are generally parallel to the direction of coil winding as shown in Fig. 2. Presence of any defect in the material such as cracks, corrosion, wall thinning or any other discontinuity which affects the electrical conductivity $(\sigma)$ and magnetic permeability $(\mu)$ of the material, causes distortion to eddy current flow and, in turn, changes the coil impedance which is a complex quantity with real (*H*) and imaginary (*V*) components.

The locus of impedance change during the movement of a probe coil over a test object is called an EC signal. While the amplitude of EC signal provides information about the severity of the defect, the phase angle wrt to lift-off (distance between coil and object surface) provides information about the depth of the defect[9]. Phase angle information of the signals is effectively used in EC testing to discriminate desired and undesired variables. Reference standard defects are used for assessing the EC test sensitivity. Calibration graphs between EC signal parameters and defect dimensions are used for sizing unknown defects.

Apart from defects, other variables such as wall thickness variations, surface roughness, edge-effect,

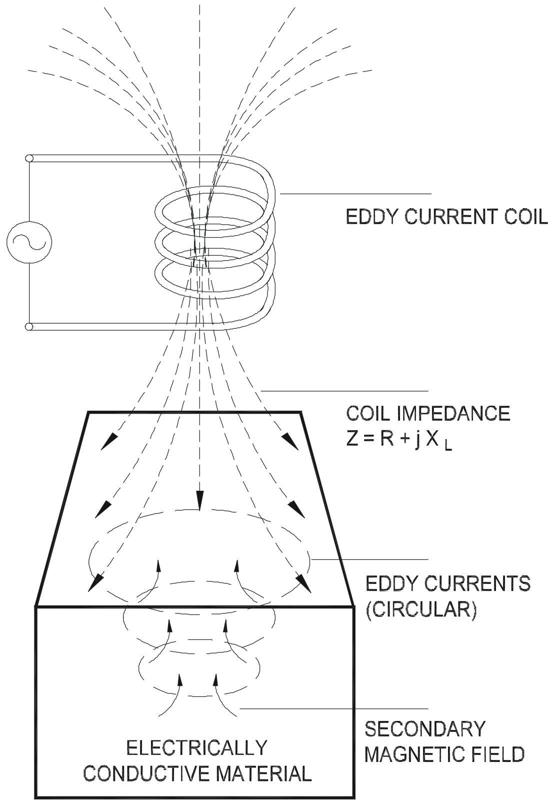


**Figure 2. Principle of eddy current testing.**

etc also influence the impedance change. It is essential to suppress the impedance changes due to these disturbing variables for successful detection and sizing of defects. Proper selection of probes and optimisation of test parameters such as test frequency, phase angle, and gain is important. In many situations, multi-frequency methods are also adopted[10]. Depth of penetration of eddy currents, in other words, the depth of inspection, is set following the classical *skin-effect* phenomenon. For conducting materials such as duralumin, lower excitation frequencies are used.

## 3. DEVELOPMENT OF EDDY CURRENT TEST PROCEDURE

For developing the eddy current test procedure, EC instrument (MIZ-20A, M/s Zetec Inc, USA) interfaced to a personal computer with facility for data acquisition, storage, and analysis was used (Fig.3). A shielded ring type EC probe (6 mm inner dia) consisting of driver/pick-up coils stacked one above another and having an operating frequency in the range of 1 kHz-20 kHz was employed. This type of probe gives very good electromagnetic coupling and minimises the operator-induced signals due to improper centering of probe over the rivet heads. During testing, the probe is kept over the rivet heads and the imaginary (*V*) component of the impedance changes during the probe lift-off are measured and analysed.

### 3.1 Specimen Details

For simulating the actual air-intake structures, six

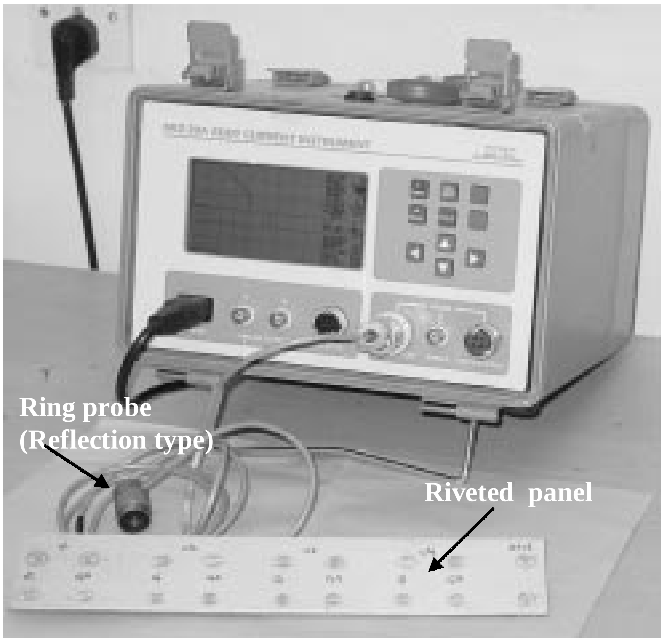


**Figure 3. Reflection type ring probe connected to EC instrument for detection of defects in countersunk regions of rivets.**

sets of riveted duralumin sheets of different thicknesses (2 or 3) were assembled. The rivets were of 4 mm and 5 mm dia. To simulate the fatigue cracks in rivets, artificial grooves (*G*) of four different depths (0.25 mm width) were machined in the countersunk regions of the rivets. Some of the grooves were filled with a mixture of aluminium powder and glue (*GA*) simulating the corrosion. The dimensional details of the panels and the grooves are given in Table 1 and the nomenclature followed for the grooves in the rivets is depicted in Fig. 4. In brief, $5_{0.75}$ refers to a 0.75 mm deep groove in a 5 mm dia rivet. The dimensions of the notches were arrived at based on the expected defects and the design considerations.

### 3.2 Experimental Details

As discussed earlier, selection of test parameters is important for minimising the interferences from undesired variables so that defects are detected reliably. Three important parameters are: test frequency, gain, and phase angle. In general, test frequency is chosen such that maximum amplitude signal is produced for defects, and at the same time, with good phase separation from interfering signals.

In this study, lift-off signal was utilised for detection. Probe was placed on a good (defect-free) rivet head and the phase angle of lift-off signal was set along the $x$-axis (real component, $H$) on the instrument screen. The test frequency, gain and phase angle in the EC instrument were optimised such that:

(i) Lift-off signal amplitude due to grooves in rivets is maximum wrt to defect-free rivets, and

(ii) Signal phase angle between grooves in rivets and defect-free rivets is maximum.

The EC probe response at different frequencies for

**Table 1. Details of machined grooves in rivet heads**

| Rivet diameter, (mm) | Layer thickness combinations, (mm) | Number of rivets | | | | Groove fill status | Panel number |
|---|---|---|---|---|---|---|---|
| | | $*4_{0.25}$ | $4_{0.5}$ | $4_{0.6}$ | $4_{0.75}$ | | |
| 4 | 1.2+2.5+1.2 | 2 | 2 | 2 | 2 | G | $S_1$ |
| | | 2 | 2 | 2 | 2 | GA | |
| | 1.5+1.2+1.5 | 2 | 2 | 2 | 2 | G | $S_2$ |
| | | 2 | 2 | 2 | 2 | GA | |
| | 1.8+1.5+1.2 | 2 | 2 | 2 | 2 | G | $S_3$ |
| | | 2 | 2 | 2 | 2 | GA | |
| | 2.0+1.5+1.2 | 2 | 2 | 2 | 2 | G | $S_4$ |
| | | 2 | 2 | 2 | 2 | GA | |
| | 2.5+1.2 | 2 | 2 | 2 | 2 | G | $S_5$ |
| | | 2 | 2 | 2 | 2 | GA | |
| | 3.5+1.2 | 2 | 2 | 2 | 2 | G | $S_6$ |
| | | 2 | 2 | 2 | 2 | GA | |
| | | $*5_{0.75}$ | $5_{1.0}$ | $5_{1.1}$ | $5_{1.25}$ | | |
| 5 | 1.2+2.5+1.2 | 2 | 2 | 2 | 2 | G | $S_7$ |
| | | 2 | 2 | 2 | 2 | GA | |
| | 1.5+1.2+1.5 | 2 | 2 | 2 | 2 | G | $S_8$ |
| | | 2 | 2 | 2 | 2 | GA | |
| | 1.8+1.5+1.2 | 2 | 2 | 2 | 2 | G | $S_9$ |
| | | 2 | 2 | 2 | 2 | GA | |
| | 2.0+1.5+1.2 | 2 | 2 | 2 | 2 | G | $S_{10}$ |
| | | 2 | 2 | 2 | 2 | GA | |
| | 2.5+1.2 | 2 | 2 | 2 | 2 | G | $S_{11}$ |
| | | 2 | 2 | 2 | 2 | GA | |
| | 3.5+1.2 | 2 | 2 | 2 | 2 | G | $S_{12}$ |
| | | 2 | 2 | 2 | 2 | GA | |

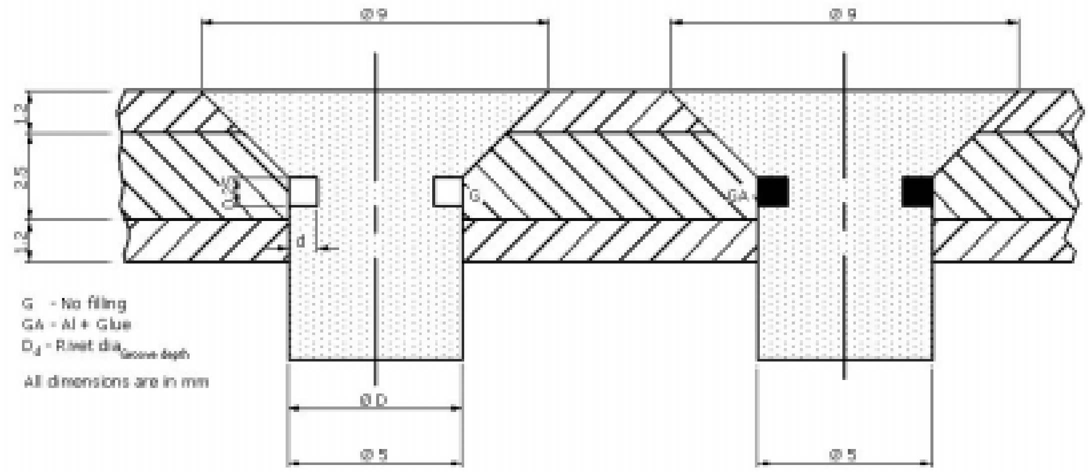


**Figure 4. Nomenclature of artificial grooves in the countersunk regions of rivets in panel S7 filled with simulated corrosion product.**

riveted panel S7 (5 mm dia rivet head) having grooves of 0.75 mm, 1.0 mm, 1.1 mm and 1.25 mm depths is shown in Fig. 5. As can be seen, at 3 kHz, the response from all the four grooves reaches a maximum. Similar response was observed for this probe placed over 4 mm dia rivets having grooves of 0.25 mm, 0.5 mm, 0.6 mm and 0.75 mm depths. In view of this, 3 kHz was chosen as optimum test frequency. The depth of penetration of eddy currents in the rivets at this frequency is about 3 mm. The instrument phase was set such that the lift-off signal from defective rivets was dominant along the vertical axis (*V*). Further, V/H ratio of 2.5 was set for selective amplification of the vertical output from defective rivets.

During EC testing of riveted panel, uniform near-zero lift-off and proper probe centering were maintained. It was observed that the responses for 4 mm and 5 mm dia rivets were different. The response was higher for 5mm dia rivets. This was expected and found to be due to very good coupling between EC probe and outer edge of the rivets. As it is preferred to use same probe for the actual inspection of 5 mm as well as 4 mm dia rivets for field implementation point of view, different gain settings that would give near-identical instrument response were tried and 20 dB and 30 dB were found to be optimum, respectively. The vertical output was measured for all the rivets in the panels at these optimised conditions and the results were analysed.

## 4. RESULTS AND DISCUSSIONS

Typical eddy current signals at optimum test conditions for defect-free rivets and for rivets under G (unfilled) and GA (filled) conditions are shown in Fig. 6. As can be observed, good phase discrimination is noticed between defect-free and defective rivets.

The difference in EC response for filled and unfilled grooves is explained with the help of universal impedance plane diagram of the EC probe shown in Fig. 7. The impedance plane diagram depicts the impedance lift-off

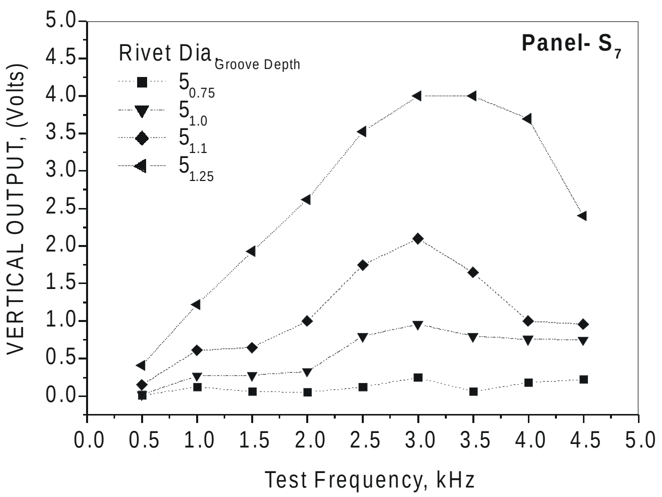


**Figure 5. Optimisation of test frequency. At 3 kHz (depth of penetration of eddy currents ~ 2 mm), EC response from grooves shows a distinct peak.**

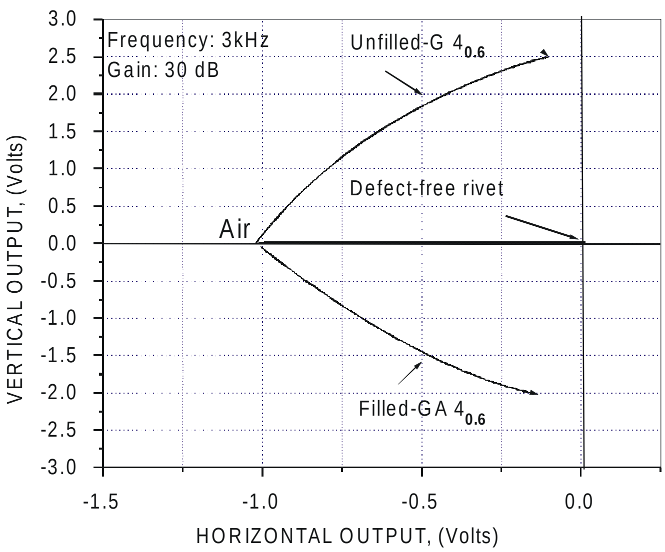


**Figure 6. Typical EC signals from 4 mm dia. defect-free rivet and rivets with filled (GA) and unfilled (G) grooves.**

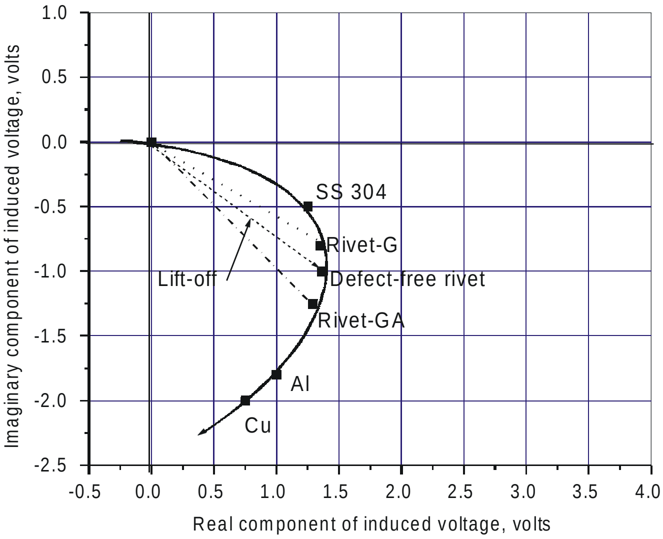


**Figure 7. Universal impedance plane diagram for reflection type ring EC probe showing the lift-off response for different electrically conducting materials.**

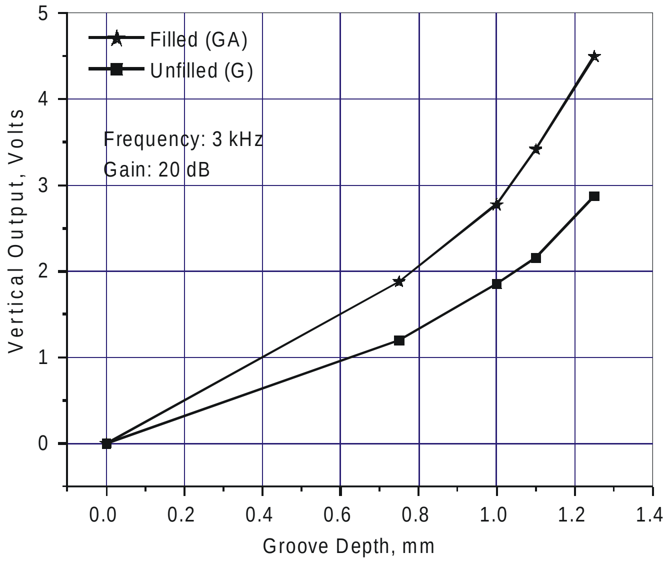


**Figure 9. EC response for 5 mm diameter rivets with unfilled and filled grooves.**

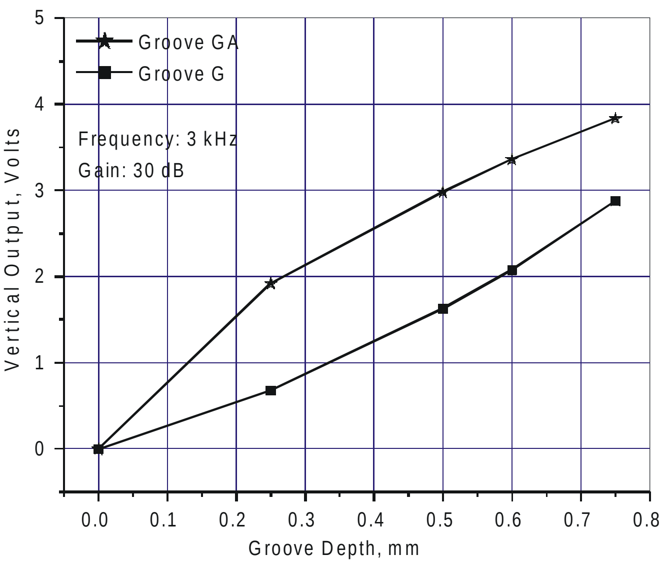


**Figure 8. EC response for 4 mm diameter rivets with unfilled and filled grooves.**

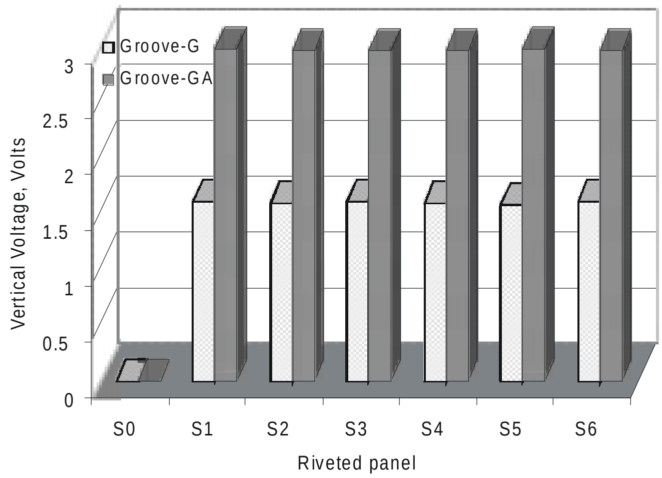


**Figure 10. Detection performance of the EC procedure for $4_{0.5}$ riveted panels with various combinations of multi-layers at optimum test conditions.**

locus of electrically-conducting materials, e.g., stainless steel, aluminium, duralumin, and copper. As the electrical conductivity increases, the impedance lift-off locus moves downwards in the impedance plane and vice-versa. In the case of unfilled grooves, the impedance lift-off locus moves upwards due to reduction in effective electrical conductivity. In contrast, the impedance lift-off locus moves downwards in the case of grooves filled with aluminium powder due to increase in effective electrical conductivity. The movement of impedance lift-off locus produces corresponding changes in EC response voltages along horizontal and vertical axes. Thus, at the optimum test conditions, it is possible to identify whether a rivet is defective at the countersunk region from the absolute amplitude of the vertical signal. Similarly, whether the defect is filled with some corrosion product, can be identified from the phase of the impedance plane signal.

The EC response for 4 mm dia rivets consisting of grooves filled with aluminium powder (*GA*) and unfilled grooves (*G*) is shown in Fig.8. Similarly, response for 5 mm dia rivet heads is given in Fig.9. As can be noted, the EC response for filled grooves is higher as compared to the unfilled grooves and this response is found to increase with the groove depth, for both 4 mm and 5 mm dia rivets. By using a threshold of 0.5 V for the absolute vertical voltage, it is possible to reliably detect 0.25mm deep defect in 4 mm dia rivets and 0.75 mm deep defect in 5 mm dia. rivets.

Figure 10 shows the detection performance of the EC procedure on various panels having same type of defect i.e. $4_{0.5}$ in different combinations of thickness layers (Table 1). The response is found to be independent of thickness of layers. This is expected, essentially, because of the fact that the depth location of the groove is same from top and the eddy currents are concentrated to the rivet head rather than in the multi-layers.

In the studies reported here, corrosion product is simulated using aluminium powder in glue matrix. However, the actual corrosion products are usually oxides, hydroxides, etc. with poor electrical conductivity. Such products would produce signals almost identical to the unfilled groove signals and this is expected to enable accurate sizing of defects, depending on the calibration reference defects. This is an interesting observation made from these experiments. This study clearly demonstrates that proper selection of probe and systematic optimisation of test parameters enable reliable detection of potential defects such as fatigue cracks and hidden corrosion in the countersunk regions of rivets and also defect sizing.

The sensitivity of the procedure to detect much shallower defects can be further enhanced using giant-magnetoresistive (GMR) sensors for receiving the magnetic fields of distorted eddy currents at defect regions in the rivets. Also, in some situations, apart from identification of defective rivets, determination of circumferential location of the defects is necessary. For such an application, the proposed procedure is inadequate and it is necessary to use spot type probes that are made to scan uniformly over the rivet-heads. Preliminary studies carried out using reflection type spot probe with a mechanical centring device have confirmed identification of circumferential location of defects.

## 5. CONCLUSIONS

An effective eddy current test procedure has been developed for reliable detection of fatigue cracks in countersunk regions of rivets in air-intake structures. Lift-off signal has been utilised to distinguish defective rivets from defect-free rivets. This procedure has resulted in reliable detection of 0.25 mm deep defects in 4 mm and 0.75 mm deep defects in 5 mm dia rivets. Using the phase of impedance plane signals, it is possible to identify if the defect is filled with corrosion product. The procedure is not affected by the thickness of the multilayers. Further, the procedure is amenable for field implementation.

## ACKNOWLEDGEMENTS

Authors thank Dr A Venugopal Reddy, Director, RCMA (Materials), Hyderabad, for useful discussions and Shri S. L. Savrekar, Chief Manager (QC), Aircraft O/H and AUR and DC, HAL, Bangalore, for providing the riveted specimens and for useful discussions. Authors are also thankful to Shri P. Krishnaiah, EMSI Section, NDE Division, IGCAR for help during the experiments.

## REFERENCES

1. Pitt, S. & Jones, R. Multiple-site and widespread fatigue damage in ageing aircraft. Engg. Failure Analy., 1997, **4**(4), 237-57.
2. Khan, M.A.U. Non-destructive testing applications in commercial aircraft maintenance.*In* Proceedings of 7th ECNDT, 1999, **4**(6).
3. Anindya, G. & Heung, S. Damage tolerance management for aircraft and rotorcraft structural components. *J. of Aircraft*, 2006, **43**(6), 1676-684.
4. Sasi, B.; Rao, B.P.C. & Jayakumar, T. Dual-frequency eddy current non-destructive detection of fatigue cracks in compressor discs of aero engine. *Def. Sci. J.*, 2004, **54**(4), 563-70.
5. David, G. M. & Floyd, W. S. Interlayer crack detection results using sliding probe eddy current procedures. *In* Proceedings of 10th APCNDT, 2001, Brisbane.
6. Fulton, J.R; Winchesld, B.; Natge, S. & Min, Namkung. Development and testing of rotating probe method for airframe rivet head inspection, *In* Review of Progress in QNDE, 1995. **14B**, Plenum Press, New York. pp 2317.
7. Don, Hagemaier & Greg, Kark. Eddy current detection of short cracks under installed fasteners. *Materials Evaluation*, 1997, **5**(1), 25-30.
8. Van der Walde, K. & Hillberry, B. M. Initiation and shape development of corrosion nucleated fatigue cracks. *Int. J. Fatigue*, 2007, **29**, 1269-281.
9. Hagemaier, D. J. Fundamentals of eddy current testing, American Society for Non-destructive Testing (ASNT). Inc. ISBN 0-931403-90-1, 1990. pp. 61.
10 Rao, B.P.C. Introduction to eddy current testing. Narosa Publishing, New Delhi, 2007.

### Contributors

**Ms B. Sasi** obtained her MSc (Applied Physics) from Gandhigram Rural Institute, Deemed University. She has been working in Indira Gandhi Centre for Atomic Research (IGCAR) in the field of development of electromagnetic non-destructive evaluation (NDE) techniques. Her areas of research include: Electromagnetic NDE, signal processing, sensor design and material characterisation.

**Dr B.P.C. Rao** heads Electromagnetics, Modelling, Sensors and Imaging (EMSI) Section, NDE Division, IGCAR. He is specialised in the area of NDE of metallic materials for detection and characterisation of defects and microstructures. He has published more than 100 research papers in various international journals and conferences.

**Dr T. Jayakumar** heads the NDE Division, IGCAR. He is specialised in the area of NDE for characterisation of defects, residual stresses and microstructures and failure analysis of engineering components. He has published more than 200 research papers in various international journals.

**Dr Baldev Raj** is Director, IGCAR, Kalpakkam. He has published more than 650 papers in several leading national and international journals in the area of metallurgy, material science and NDE. He has authored and edited 38 books. He is a fellow of several national and international academies and societies and is a recipient of many national and international awards.